Constant Curvature Kinematic Model Analysis and Experimental Validation for Tendon Driven Continuum Manipulators

S. Mosqueda[1], Y. Moncada[1], C. Murrugarra[1] and H. León-Rodriguez[1,2]
[1]*Electronic Engineering Program, El Bosque University, Bogota, Colombia*
[2]*Bioengineering Program, El Bosque University, Bogota, Colombia*

Keywords: Robotic, Kinematic, Continuum, Workspace, Tracking, End Effector, Mathematical Model.

Abstract: In this paper an analysis is done to the current kinematic model for continuum robot, with the goal of determining the accuracy of the experimental validation of the constant curvature kinematic model to establish a relation between the mathematical model and continuum robot, and its feasibility of applying for any type of continuum structure, measuring the end effector planar trajectory based on the displacement of passive cables located along the structure. To test the kinematic model, a prototype of continuous robot composed of 1 segment with 7 sections, controlled by 3 cables, per section was fabricated, we also propose a modular segment (link) with free joints, the modularity allows to extend the length of the segment and also allows to add segments and connect in the form of serial chain and describe the radius of concave and/or convex curvature and allow the robot manipulator to follow different trajectories and displacements in their workspace. The kinematic model of constant curvature used in continuous robots with minimal positioning errors was implemented and tested.

1 INTRODUCTION

The robotics field is ever-growing and developing, always looking for ways to provide solutions for specific needs; in the beginning, research was mainly focused automated manipulators that could take the place of humans in dangerous work environments or manufacturing processes, especially in those were efficiency meant executing a task over and over, always in the same time. Industrial robots have traditionally consisted of a serial like to connect joints directly actuated (Pires, 2007), although these types of robots have been proved to be useful in many scenarios, they have obvious drawbacks in more constricted spaces due to the lack of compliance generated by the low level of flexibility and degrees of freedom (D.O.F.), and in real-world scenarios and situations that are not pre-choreographed, it is generally not feasible to use the rigid link manipulator.

Many of these problems have been resolved through biologically inspired designs, which aim to copy the movement properties and adaptability of certain animal extremities such as octopus, or squid tentacles (Laschi et al., 2012), (McMahan et al., 2006), elephant trunks (Tiefeng et al., 2015) and snake-like structures (Crespi et al., 2005). This type of mechanism known as a continuum or hyper-redundant robots differs from traditional manipulators in the sense that they are capable of possessing a high range of flexibility and more degrees of freedom enabling them to traverse precisely through almost any ”space” and around many obstacles. Hence, they are considered to be ideal for probing cramped and hazardous industrial environments, as they can be used to inspect nuclear reactors (Ma et al., 1994), as well as confined spaces (Liu et al., 2016), to search and rescue in disaster situation (Meng et al., 2013), and in recent years, they have gained wide interest from the medical field (Burgner-Kahrs et al., 2015), specifically, in conducting Minimal invasive surgery (MIS) (Burgner et al., 2014).

This type of robots can be classified by a defining feature, which is a continuously curving backbone or core, its shape can be modified with diverse types of actuated mechanism, tendon mechanism (Li et al., 2016) or pneumatic mechanism (Mahl et al., 2014); this backbone, even though it is known as continuous as it can be segmented, compromised of a series of rigid-links, which together give the appearance of a continuous structure. One of the best examples of this can be seen in a development done by the British company OC robotics (Robotics OC, 2016).

Mosqueda, S., Moncada, Y., Murrugarra, C. and León-Rodriguez, H.
Constant Curvature Kinematic Model Analysis and Experimental Validation for Tendon Driven Continuum Manipulators.
DOI: 10.5220/0006913502110218
In *Proceedings of the 15th International Conference on Informatics in Control, Automation and Robotics (ICINCO 2018) - Volume 2*, pages 211-218
ISBN: 978-989-758-321-6

Most continuum robots can also be known as under-actuated since they have fewer actuators than DOFs. these under-actuated systems allow for a significant simplification of the control system, with the disadvantage that some workspace is lost due to the reduce dexterity. With this in mind, we can further classify these robots by their type of actuation and structure, in three main categories, Tendon-driven, concentric tube and locally actuated(Walker, 2013), also known in the literature as tendon-driven continuum manipulators (TCM), tendon-driven serpentine manipulators (TSM) and concentric tube manipulators (CTM)(Li et al., 2017).

With the goal of obtaining a reliable kinematic model, capable of accurately describing the behavior of any continuum robot first we have to review what developments have been made so far, starting from the proposal of clothoid curves for mimicking a snake's locomotion (Hirose, 1995), followed by the work of Chirikjian and Burdick that extended on this approach of fitting the hyper-redundant robot to analytical desirable mathematical curves by establishing them as the product of a Bessel function with sines and cosines (Chirikjian and Burdick, 1995b), furthermore, they described the behavior of the constant curving structure using the Frenet-Serret Frames equations (Chirikjian and Burdick, 1995a). Subsequently, the work of Walker (Jones and Walker, 2006), Zheng, Webster and Jones (Webster and Jones, 2010) allowed for the integration of these models, with the D-H parameters (Hannan and Walker, 2003), the integral representation and a product of exponentials (POE)(Li et al., 2017), to finally derive the constant-curvature kinematic model, which is one of the most well-known and used for modeling continuum robots.

In this work we aim to do an experimental validation of the constant-curvature kinematic model to establish a relation between the mathematical model and continuum robot, measuring the end effector planar trajectory based on the displacement of passive cables located along the structure, with the purpose of estimating the resulting shape of the planar trajectory, a video processing software was used.

This paper presents the Introduction as the first section, then a formal description of the Mathematical model, followed by the description of the Experimental Setup explaining the technical characteristics of construction of the continuous robot, motion, and measurements, we continue with the Results and finally the Conclusions.

2 MATHEMATICAL MODEL

This section defines the kinematic model that will be applied to describe the manipulator shape and end-effector position. As mentioned in the introduction, a robust kinematic model based on constant curvature, seems to be the best option for describing the movements of a continuous structure.

According to classical robotics, modeling of an articulated system, consist of determining the position and orientation of the end effector, regarding a system of reference coordinates at the base of it, this can be achieved by defining a robot as a set of rigid elements or link joints, however, this method is not applicable to a system that has more degrees of freedom than those needed to carry out a basic task, as is the case with continuous robots.

This kinematic model, developed (Jones et al., 2006) and (Chirikjian and Burdick, 1995a), uses a series of substitutions on the Denavit-Hartenberg (D-H) transformation matrix, in order to obtain a model that defines a more approximate behavior, where a standard homogeneous transformation matrix $A(\theta,d)$ is used to describe a series of independent translations and rotations. The latter requires a different mathematical analysis, in which a series of substitutions are made on the D-H transformation matrix, in order to obtain a model that relates a more approximate behavior. The conventional notation involving a homogeneous matrix is yielded by $A(\theta,d)$, where: θ represents the independent rotations of the joints and d the translations. However, for continuous robots, performing this analysis involves a homogeneous matrix for each section that makes up a segment, so authors such as Ian D. Walker, which associates the shape of the robot with a curve in space by the middle of the Frenet Serret equations (DHB, 2013), one can establish an equivalent to rotations and translations. Thus, the

$$A=\begin{bmatrix} \cos^2(\phi)[\cos(ks-1)]+1 & \sin(\phi)\cos(\phi)[\cos(ks-1)] & -\cos(\phi)\sin(ks) & \frac{cos(\phi)[\cos(ks-1)]}{k} \\ \sin(\phi)\cos(\phi)[\cos(ks-1)] & \cos^2(\phi)[\cos(ks-1)]+\cos(ks) & -\sin(\phi)\sin(ks) & \frac{sin(\phi)[\cos(ks-1)]}{k} \\ \cos(\phi)\sin(ks) & \sin(\phi)\sin(ks) & \cos(ks) & \frac{\sin(ks)}{k} \\ 0 & 0 & 0 & 1 \end{bmatrix} \quad (1)$$

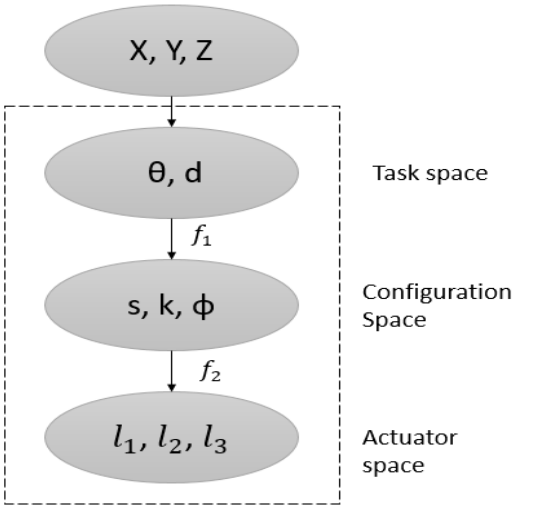

Figure 1: The space transformations between the D-H parameters and s, k , ϕ, l_1, l_2 and l_3.

first step to obtaining a reliable mathematic model, is to establish a relationship between the D-H parameters θ, and the trunk parameters s, k, ϕ, and from this, obtaining a more approximate approach to the continuum robot movements in terms of the cable length (Jones and Walker, 2006), (Webster and Jones, 2010). The space transformations between the D-H parameters and s, k, ϕ and l_i, as shown in Figure.1.

According to the coordinate system and the geometric relationship with the *arc* parameters, the homogeneous matrix of the n segment can be calculated as Eq.1, where the matrix of transformation A, allows us to know the position and orientation to perform an analysis of the bending of the continuum robot of the end effector and its workspace $(3D)$. In Eq.2, the space position of the end effector and Eq.3, get the bending performance on 2D with the matrix.

$$\begin{bmatrix} P_x \\ P_y \\ P_z \end{bmatrix} = \begin{bmatrix} \frac{\cos(\phi)[\cos(ks-1)]}{k} \\ \frac{\sin(\phi)[\cos(ks-1)]}{k} \\ \frac{sin(ks)}{k} \end{bmatrix} \tag{2}$$

$$\begin{bmatrix} P_x \\ P_y \\ P_z \end{bmatrix} = \begin{bmatrix} \frac{\cos(ks-1)}{k} \\ 0 \\ \frac{sin(ks)}{k} \end{bmatrix} \tag{3}$$

Through equations Eq.4, Eq.5 and Eq.6, we can find the position of the end effector in regard to the *arc* parameters, these parameters can be controlled by adjusting the length of the tensor cables, therefore, its necessary to derive the mapping from the linear actuators length to the *arc* parameters.

$$\phi = \tan^{-1}\left(\frac{\sqrt{3}}{3}\cdot\frac{l_3+l_2-2l_1}{l_2-l_3}\right) \tag{4}$$

$$k = 2\frac{\sqrt{l_1^2+l_2^2+l_3^2-l_1l_2-l_2l_3-l_1l_3}}{d(l_1+l_2+l_3)} \tag{5}$$

$$s = \frac{l_1+l_2+l_3}{3} \tag{6}$$

Finally, establish a connection to obtain the position of the end effector in relation to the cable lengths, we must know the following parameters from a section of the manipulator; the length of one of its segments, the curvature of the section (k), the angle at which the curvature (ϕ) is found, the distance from the center of the manipulator to the location of the cables (s), and the number of segments in the manipulator section (n); with these parameters we obtain the Eq.7.

$$\begin{bmatrix} l_1 \\ l_2 \\ l_3 \end{bmatrix} = \begin{bmatrix} s\left[1-kd\sin(\phi)\right] \\ s\left[1+kd\sin\left(\frac{\pi}{3}+\phi\right)\right] \\ s\left[1-kd\cos\left(\frac{\pi}{6}+\phi\right)\right] \end{bmatrix} \tag{7}$$

3 EXPERIMENTAL SETUP

The experimental platform for Continuum Robot Manipulator is shown in Figure.2.

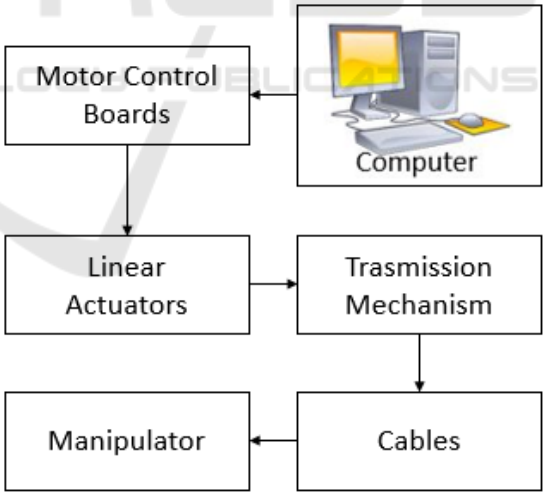

Figure 2: The experimental platform for Continuum Robot Manipulator.

The Continuum Robot Manipulator system was implemented by:

1. *Processing central* by a computer.
2. *Motor Control Boards* using the three Phidget motor control (1065),

3. *Linear Actuators and Transmission Mechanics* by three ECO-WORTHY: stroke length 150mm, rated at 5.7mm/s, 1500N pull and 1200N push force with magnetic encoder.
4. *Cables* wire, stainless-steel (316), with 0.28m in length and 3.00mm in diameter.
5. *Manipulator* one segment in PVC with 0.22m in length and 0.08m in diameter, with seven sections, free joints.

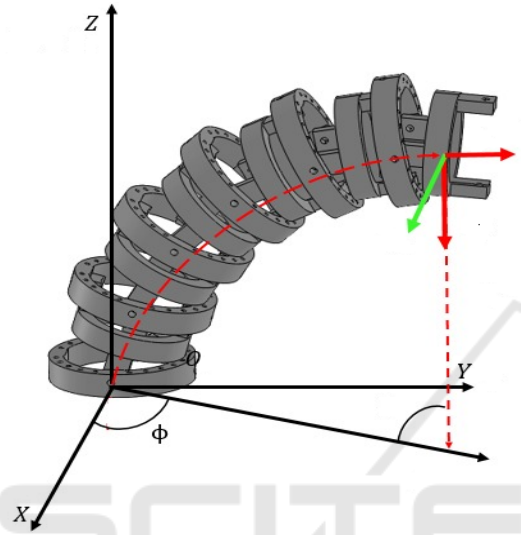

Figure 3: The Continuum Robot Manipulator composed of 1 segment, 6 sections and free joints between sections.

Figure.3, shows a computer rendering of the manipulator prototype, composed of 1 segment, 7 sections and free joints between sections. Figure.4, shows a computer rendering of the robotic extended prototype, where of the manipulator is composed of 2 segments, 14 sections, 6 cables (3 for each segment), and 6 linear actuators, one for each cable.

The kinematic model used to obtain the necessary cable lengths to move the manipulator to a certain position was simulated with MATLAB, using the equations of the section 2. To start the experimental validation, first we chose a position in the X, Z plane, that we wanted the end effector to be in, then, we proceeded to reposition the motors using the Motor Control Boards until the lengths of the tension cables in the experimental prototype were as close as possible to the theoretical lengths, in order to compare the final position of the actuator.

4 RESULTS

Figure.5, shows the evaluation of the mathematical model for a continuum robot manipulator implemen-

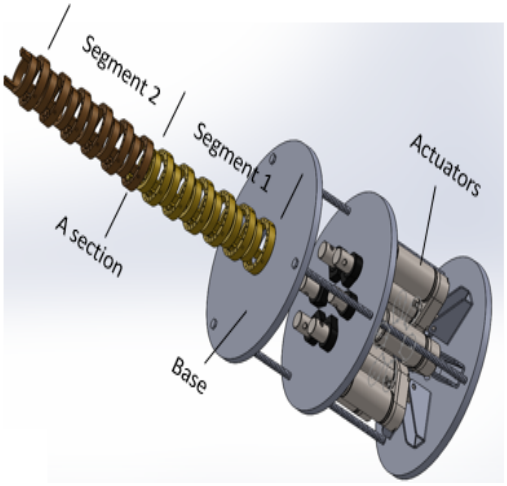

Figure 4: Design of the Continuum Robot: composed of 2 segments, 14 sections, 6 cables (3 for each segment), and 6 linear actuators.

ted in this work, $1segment = 0.220m$.

Figure.6, shows the continuum robot manipulator (1 segment) implemented for an experimental position obtained using the kinematic model and calculate the medium squared error and find out how accurate is the mathematical model, the position of the end-effector was acquired using the Tracker video analysis and modeling tool software.

To validate the mathematical model, a series of experiments were performed, in these tests, the max values of *arc* parameters were measured during planned movements of the manipulator with the following conditions: $\phi = 0$, s = constant value = $0.220m$, and a maximum value of $k = \frac{1}{0.14m}$, obtaining the magnitudes of the lengths of the cables with Eq.7.

Using the video Tracker software and bright colored markers to get a better recognition of the robot segments, 3 tests were run, in each one, the movement values of $X(m)$ y $Z(m)$ was recorded. Different test experiments were performed as the one on Figure.7, under some values of calculated for l_1, l_2, l_3, and Figure 8, shows one of the results of tracking the movements previously described, in this case, to be consistent with the variables used, for this figure the "X" axis is the "Z" axis corresponding to our nomenclature.

From Table.1, through the measuring of the cable lengths, calculating the curvature of the end effector and comparing it to the theoretical model, where: k_{theo} is obtained by the mathematical model and k_{exp} is the measure in the experimental setup implemented. To further evaluate the tracking performance of 3 tests, the Root Mean Square Error (RMSE) is used as follows for each one of them.

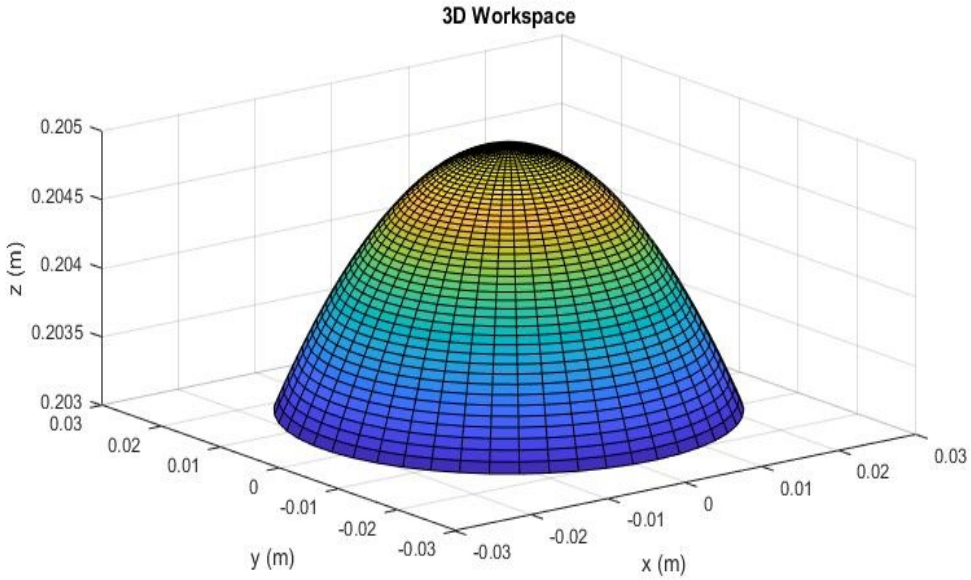

Figure 5: 3D Workspace defined by the mathematical model for Continuum Robot Manipulator with dimensions of the manipulator whit length=0.220m.

Figure 6: Moving Robot positioning using Tracker software.

$$RSME = \sqrt{\frac{1}{n}\sum_{i=1}^{n}(\|Z_{theo} - Z_{exp}\|)^2} \qquad (8)$$

where n is a given time for taking samples, n is the total number of samples in that given time, Z_{theo}, is the desired trajectory and Z_{exp}, is the measured trajectory. In the experiments javascript:void(0);conducted we took n=82 samples during the period of 2.7 minutes.

From Table2, we can see that the RMSE is well within the normal and functional values and that this error can very well be caused by mechanical imperfection in the prototype.

Table 1: Experimental Results: Calculating the curvature of the end effector in the experimental setup and comparing it to the theoretical model.

$l_1(m)$	$l_2(m)$	$l_3(m)$	$k_{theo}(m)$	$k_{exp}(m)$
0.20	0.20	0.20	Ind	Ind
0.20	0.24	0.16	0.14	0.13
0.20	0.22	0.14	0.20	0.18

Table 2: Experimental Results: Evaluate the tracking performance using RMSE comparison by the desired trajectory and measured trajectory in three tests and μ (mean or arithmetic average) .

$Test1$ (m)	$Test2$ (m)	$Test3$ (m)	μ
0.0156	0.0352	0.0016	0.0023

The results shown in Figure.9, illustrate the tracking performance in terms of the RMSE of all the experiments, their average and the calculated trajectory. As we can see, the RMSE reaches to 0.015 m (0.0153 m to 0.035 m) in the open-loop case, whereas the RMSE decreases to only 0.05 m with the measured trajectories average.

5 CONCLUSION

In this paper the mathematical model in the space transformations between the D-H parameters and s, k , ϕ, l_1, l_2 and l_3 was implemented and tested the constant curvature kinematic model currently used in most continuum robot manipulators, and from the re-

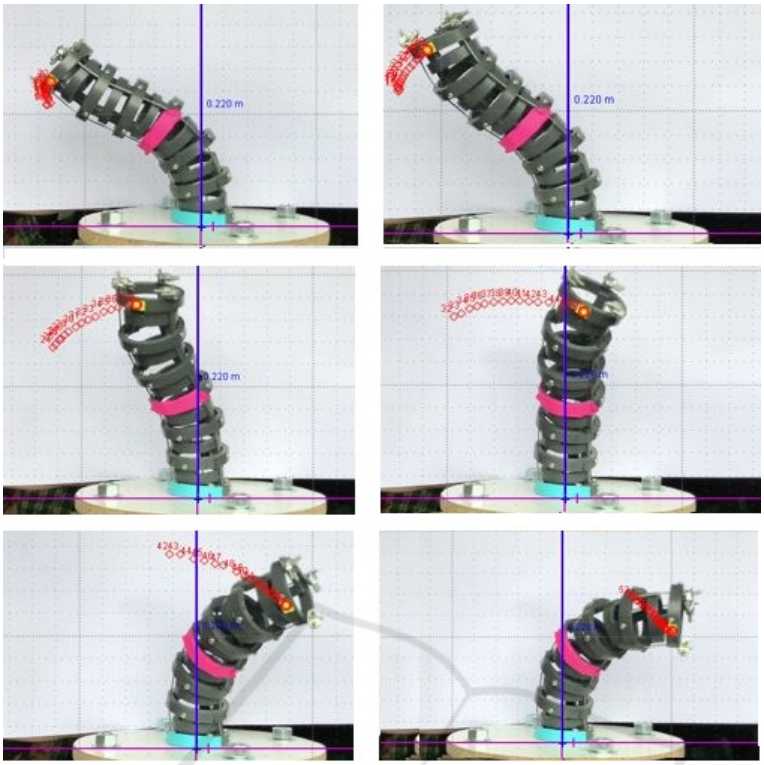

Figure 7: Tracking Position of Robot Continuum using video Tracker.

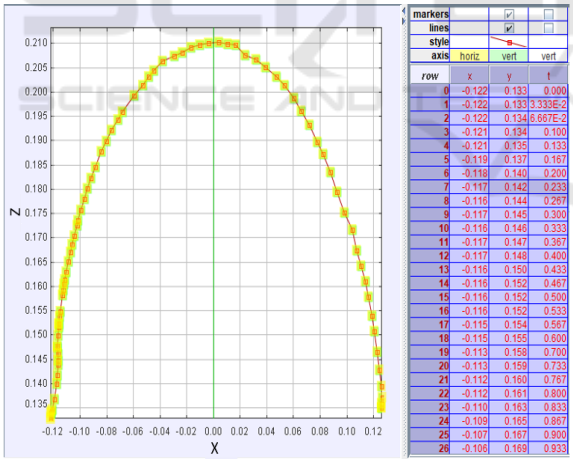

Figure 8: Tracking Position of Robot Continuum using video Tracker: Bending Movement Results

sults we concluded that it is possible to implement a continuum robot structure with minimal positioning errors, however, it must be taken into account that adding more segments to the robot will increase the complexity of the system due to the increase in the number of cables and actuators in the system.

A modular continuum robot manipulator was proposed, whose length can be extended by adding sections to the segments (links) and, in turn, define new configurations by extending the length of the manipulator by adding new segments. This functionality would allow the continuum robot manipulator to track trajectories in the combination of a concave and convex radius of curvature that could be used to perform spatial shifts and obstacle avoidance. Another advantage of the design of the segments of this robot manipulator is that it is built with fairly light material and allows to scale its cross-sectional area, which can be used in different applications, either for guided searches in disaster areas or for applications of health. The experimental setup allowed to validate the mathematical model and identify the proposed modular link design.

ACKNOWLEDGEMENTS

This work is supported by a grant from the El Bosque University and the Research Vice-rectory with the project number PCI-2017-8832.

The authors would like to thanks to the Professor Michal Canu for his constant aid in the control aspect.

The authors also wish to thank the Electronic Engineering and Bioengineering programs of the Faculty of Engineering of El Bosque University for all the support received.

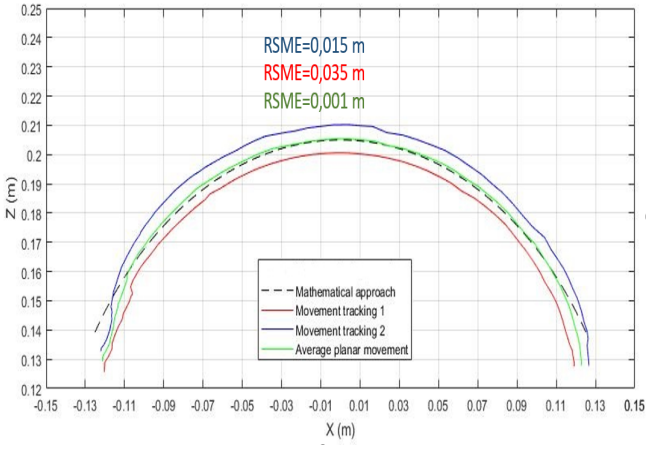

Figure 9: Comparison between different movements, their average and the calculated trajectory.

REFERENCES

Burgner, J., Rucker, D. C., Gilbert, H. B., Swaney, P. J., Russell, P. T., Weaver, K. D., and Webster, R. J. (2014). A telerobotic system for transnasal surgery. *IEEE/ASME Transactions on Mechatronics*, 19(3):996–1006.

Burgner-Kahrs, J., Rucker, D. C., and Choset, H. (2015). Continuum Robots for Medical Applications: A Survey. *IEEE Transactions on Robotics*, 31(6):1261–1280.

Chirikjian, G. S. and Burdick, J. W. (1995a). Kinematically Optimal Hyper-Redundant Manipulator Configurations. *IEEE Transactions on Robotics and Automation*, 11(6):794–806.

Chirikjian, G. S. and Burdick, J. W. (1995b). The Kinematics of Hyper-Redundant Robot Locomotion. *IEEE Transactions on Robotics and Automation*, 11(6):781–793.

Crespi, A., Badertscher, A., Guignard, A., and Ijspeert, A. J. (2005). AmphiBot I: An amphibious snake-like robot. *Robotics and Autonomous Systems*, 50(4):163–175.

DHB (2013). Differential Geometry. *Reading*, (4):0.

Hannan, M. W. and Walker, I. D. (2003). Kinematics and the implementation of an elephant's trunk manipulator and other continuum style robots. *Journal of Robotic Systems*, 20(2):45–63.

Hirose, S. (1995). Biologically Inspired Robots: Snake-Like Locomotors and Manipulators. *Applied Mechanics Reviews*, 48(3):B27–B27.

Jones, B. A., McMahan, W., and Walker, I. D. (2006). Practical Kinematics for Real-Time Implimentation of Continuum Robots. *IEEE International Conference on Robotics and Automation*, pages 1840–1847.

Jones, B. A. and Walker, I. D. (2006). Kinematics for multisection continuum robots. *IEEE Transactions on Robotics*, 22(1):43–55.

Laschi, C., Cianchetti, M., Mazzolai, B., Margheri, L., Follador, M., and Dario, P. (2012). Soft robot arm inspired by the octopus. *Advanced Robotics*, 26(7):709–727.

Li, Z., Ren, H., Chiu, P. W. Y., Du, R., and Yu, H. (2016). A novel constrained wire-driven flexible mechanism and its kinematic analysis. *Mechanism and Machine Theory*, 95:59–75.

Li, Z., Wu, L., Ren, H., and Yu, H. (2017). Kinematic comparison of surgical tendon-driven manipulators and concentric tube manipulators. *Mechanism and Machine Theory*, 107(September 2016):148–165.

Liu, S., Yang, Z., Zhu, Z., Han, L., Zhu, X., and Xu, K. (2016). Development of a dexterous continuum manipulator for exploration and inspection in confined spaces. *Industrial Robot: An International Journal*, 43(3):284–295.

Ma, S., Hirose, S., and Yoshinada, H. (1994). Development of a hyper-redundant multijoint manipulator for maintenance of nuclear reactors. *Advanced Robotics*, 9(3):281–300.

Mahl, T., Hildebrandt, A., and Sawodny, O. (2014). A Variable Curvature Continuum Kinematics for Kinematic Control of the Bionic Handling Assistant. 30(4):1–15.

McMahan, W., Chitrakaran, V., Csencsits, M., Dawson, D., Walker, I. D., Jones, B., Pritts, M., Dienno, D., Grissom, M., and Rahn, C. D. (2006). Field trials and testing of the OcotArm continuum manipulator. *Proceedings of the 2006 IEEE international conference on robotics and automation (ICRA)*, (May):2336–2341.

Meng, G. Z., Yuan, G. M., Liu, Z., and Zhang, J. (2013). Forward and Inverse Kinematic of Continuum Robot for Search and Rescue. *Advanced Materials Research*, 712-715:2290–2295.

Pires, N. (2007). Robot Manipulators and Control Systems. *Industrial Robots Programming. Building Applications for the Factories of the Future*.

Robotics OC (2016). LaserPipe Remote in-bore laser welding of industrial pipelines.

Tiefeng, S., Libin, Z., Mingyu, D., Guanjun, B., and Qinghua, Y. (2015). Fruit harvesting continuum manipulator inspired by elephant trunk. *International Journal*

of Agricultural and Biological Engineering, 8(1):57–63.

Walker, I. D. (2013). Continuous Backbone Continuum Robot Manipulators. *ISRN Robotics*, 2013:1–19.

Webster, R. J. and Jones, B. A. (2010). Design and kinematic modeling of constant curvature continuum robots: A review. *International Journal of Robotics Research*, 29(13):1661–1683.